Numerical Analysis of Plasma Acceleration Driven by Loop Coil in Electrodeless Thruster

IEPC-2019-A-573

Presented at the 36th International Electric Propulsion Conference
University of Vienna, Austria
September 15-20, 2019

Yudai Yamakawa*, Masayuki Takahashi†, and Naofumi Ohnishi‡
Tohoku University, Sendai, 980-8579, Japan

Role of the Lorentz force on the electromagnetic acceleration mechanism in an electrodeless plasma thruster driven by a loop coil was numerically investigated. The interaction between the plasma and the electromagnetic (EM) field was reproduced, and the Lorentz force principally accelerated the plasma at the surface of the plasma where the rotating motion of electrons was induced. However, at the central region of the plasma, the Lorentz force did not work as the main acceleration mechanism because rotating electrons induced the EM field which reversed the penetrating field. The scale of this reversed field was determined by the plasma density and applied frequency, and should be a parameter for the geometry of the thruster.

Nomenclature

n	= number density
$\mathbf{v}$	= velocity
$\nu_{\rm en}, \nu_{\rm in}$	= elastic collision frequencies of electron-background gas and ion-background gas
q	= elementary charge
m	= mass
$\widetilde{\mathbf{E}}$	= electric field
$\widetilde{\mathbf{B}}$	= magnetic field
$\mathbf{j}_{\rm c}$	= current density inside the coil
$\mathbf{j}_{\rm p}$	= plasma current density
μ_0	= permittivity of vacuum
ε_0	= permeability of vacuum
c	= speed of light
$A_{\rm coil}$	= cross-section of the coil
j_0	= amplitude of the current density
f	= frequency
t	= time
r	= radial coordinate
z	= axial coordinate
θ	= azimuthal coordinate
j, k, l	= radial and axial grid position, and time step

*Graduate student, Department of Aerospace Engineering, yyamakawa@rhd.mech.tohoku.ac.jp
†Associate Professor, Department of Aerospace Engineering, mtakahashi@rhd.mech.tohoku.ac.jp
‡Professor, Department of Aerospace Engineering, ohnishi@rhd.mech.tohoku.ac.jp

I. Introduction

Electric thrusters obtain the thrust by electrically accelerating and exhausting a propellant gas in a form of high density plasma. However, most of conventional electric thrusters have a problem of an operation-time limitation. This issue is caused by an electrodes erosion at plasma generation and acceleration parts where high-energy charged particles collide against electrodes. In order to overcome this problem, some kinds of electrodeless plasma thrusters have been proposed. Electrodeless plasma thrusters are devices which generate, accelerate, and exhaust plasma without the direct physical contact between the plasma and electrodes. There are a number of electrodeless acceleration mechanisms[1]; however, practical methods have not yet established due to the complexity and difficulty of the process of the momentum transfer from electromagnetic (EM) field to the plasma.

In this study, we numerically investigate an electrodeless plasma thruster driven by a loop coil[2]. The main acceleration mechanism of this thruster is considered to be the electromagnetic force, the Lorentz force between azimuthal current inside the plasma and magnetic field. Previous study have shown the posibility that the behavior of the accelerated charged particles is based on the other several mechanisms depending on the radial position of the thruster tube[3]. In order to optimize the plasma acceleration, it needs to specify the mechanisms behind the composite acceleration-phenomenon and identify where each mechanism is dominant.

Therefore, this study is dedicated to numerically investigate the role of the Lorentz force for the plasma acceleration.

II. Thruster Concept

Electrodeless plasma thrusters consist of the plasma generation part, acceleration part, and magnetic nozzle (MN) (Fig. 1). There are some methods which accelerate the plasma without any electrode contacting with the plasma. A thruster driven by a loop coil is one of them. Once an alternating current (AC) is applied to the coil insulated from the plasma by a glass tube, electrons in the plasma react to the variable magnetic field due to the EM induction, leading to an azimuthal current (j_θ). The Lorentz force between j_θ and the radial component of MN ($B_{\mathrm{MN},r}$) accelerates electrons axially. This electrons motion generates the electric field which drives ions to the same direction as electrons. The electrons and ions are finally exhausted outside together, and the thrust is produced electromagnetically.

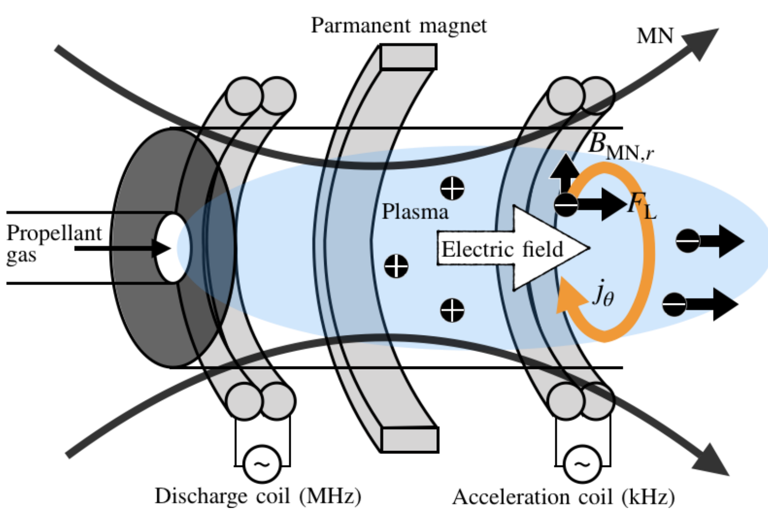

Figure 1. Schematic of electrodeless plasma thruster driven by a loop coil.

III. Numerical Method

The plasma in the acceleration part is assumed to consist of two fluids for electron and ion in order to obtain macroscopic quantities such as number density and velocity of charged particles. Because the plasma interacts strongly with the EM field, the time evolution of the EM field is also numerically solved along with the plasma fluid model.

A. Modeling

Plasma fluid model

In the plasma model, the equation of continuity and equation of motion for electron and ion are numerically solved to reproduce the plasma motion in the thruster tube:

$$\frac{\partial n_{\mathrm{e,i}}}{\partial t} + \nabla \cdot \left(n_{\mathrm{e,i}} \mathbf{v}_{\mathrm{e,i}} \right) = 0, \tag{1}$$

$$\frac{\partial \mathbf{v}_{\mathrm{e}}}{\partial t} + \nu_{\mathrm{en}} \mathbf{v}_{\mathrm{e}} = -\frac{q}{m_{\mathrm{e}}} \left(\widetilde{\mathbf{E}} + \mathbf{v}_{\mathrm{e}} \times \mathbf{B}_{\mathrm{total}} \right), \tag{2}$$

$$\frac{\partial \mathbf{v}_{\mathrm{i}}}{\partial t} + \nu_{\mathrm{in}} \mathbf{v}_{\mathrm{i}} = \frac{q}{m_{\mathrm{i}}} \widetilde{\mathbf{E}}, \tag{3}$$

where the Lorentz force $\mathbf{F}_{\mathrm{L}} = \mathbf{v}_{\mathrm{e}} \times \mathbf{B}_{\mathrm{total}}$ is induced by the total magnetic field $\mathbf{B}_{\mathrm{total}} = \widetilde{\mathbf{B}} + \mathbf{B}_{\mathrm{MN}}$ and $v_{\mathrm{e},\theta}$ induced by the coil due to the EM induction. The variable electric and magnetic fields are obtained from the EM model. In order to reproduce the more realistic phenomenon in the thruster, a source term should be included in the continuity equations because the past experiment suggested that the plasma density increased even by the acceleration coil and the change of density also contributes to the plasma acceleration mechanism. However, we omit the source term in order to focus on the Lorentz force as the main acceleration factor in this paper.

EM field model

The Maxwell's equation is numerically solved using a finite-difference time-domain (FDTD) method in order to describe the interaction between the EM field and plasma[4]:

$$\nabla \times \widetilde{\mathbf{E}} = -\frac{\partial \widetilde{\mathbf{B}}}{\partial t}, \tag{4}$$

$$\frac{1}{\mu_0} \nabla \times \widetilde{\mathbf{B}} = \mathbf{j}_{\mathrm{c}} + \mathbf{j}_{\mathrm{p}} + \varepsilon_0 \frac{\partial \widetilde{\mathbf{E}}}{\partial t}. \tag{5}$$

The EM model is coupled with the plasma fluid model via the plasma current density obtained by

$$\mathbf{j}_{\mathrm{p}} = -q \left(n_{\mathrm{e}} \mathbf{v}_{\mathrm{e}} - n_{\mathrm{i}} \mathbf{v}_{\mathrm{i}} \right). \tag{6}$$

The field components ($\widetilde{E}_\theta, \widetilde{B}_z$, and $\widetilde{B}_r$) are induced by applying the following azimuthal current density inside the loop coil to the region corresponding to the coil:

$$j_{\mathrm{c},\theta}(t) = \begin{cases} \frac{1}{2} j_0 \left(1 - \cos \frac{\pi t}{T_\omega} \right) \sin 2\pi f t & (0 \leq t \leq T_\omega), \\ j_0 \sin 2\pi f t & (T_\omega \leq t), \end{cases} \tag{7}$$

where T_ω is the starting period and is set to $2/f$ in this paper. The other components ($\widetilde{E}_r, \widetilde{E}_z$, and $\widetilde{B}_\theta$) are induced by only the radial and axial components of the plasma current.

Discretization method

The equation of motion for electrons including the Lorentz force is numerically integrated in time as follows[5]:

$$\mathbf{v}_\mathrm{e}\big|^{l+1/2} = -\, \mathbf{v}_\mathrm{e}\big|^{l-1/2} + 2\zeta[\mathbf{b}]^{-1}\mathbf{w}, \tag{8}$$

where

$$[\mathbf{b}] = \begin{pmatrix} \zeta & -b_z & 0 \\ b_z & \zeta & -b_r \\ 0 & b_r & \zeta \end{pmatrix}, \tag{9}$$

$$\mathbf{w} = \frac{1}{\zeta}\left(\mathbf{v}_\mathrm{e}\big|^{l-1/2} - \frac{q\Delta t}{2m_\mathrm{e}}\, \widetilde{\mathbf{E}}\Big|^{l} \right), \tag{10}$$

$$\begin{pmatrix} b_r \\ b_\theta \\ b_z \end{pmatrix} = -\frac{q\Delta t}{2m_\mathrm{e}}\mathbf{B}_\mathrm{total}, \tag{11}$$

$$\zeta = 1 + \frac{\nu_\mathrm{en}\Delta t}{2}. \tag{12}$$

Because the field components are defined on the staggered grid (Fig. 2), the space interpolation in consideration of the curvature is applied when Eq. (8) is updated.

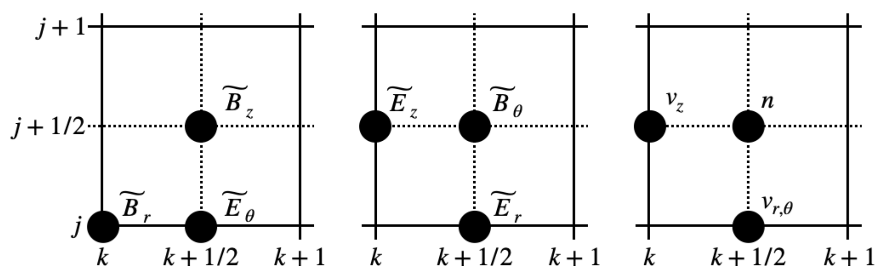

Figure 2. Components of plasma and EM field defined on staggered grid.

B. Conditions

Assuming that the phenomenon in the thruster is symmetry about an axis, the two-dimensional axisymmetric coordinate system is used for reducing the calculation costs. The plasma of $n_\mathrm{e} = n_\mathrm{i} = 10^{17}$, 10^{18}, or 10^{19} m^{-3} is set in the region of $0 \leq r \leq 10$ mm as the initial condition. Argon gas is assumed as the propellant. The ellastic collision frequencies $\nu_\mathrm{en} = 2.0 \times 10^8$ Hz for electron and $\nu_\mathrm{in} = 2.0 \times 10^6$ Hz for ion are utilized. The position of the center of the loop coil is selected as $(r, z) = (20\ \mathrm{mm}, 0\ \mathrm{mm})$ and the cross-section is $A_\mathrm{c} = 10 \times 10$ mm^2. $B_{\mathrm{MN},r}$ whose peak is 0.01 T at $z = 0$ mm is set assuming only the radial component of the MN which produces the axial Lorentz force. The AC of 300 A$_\mathrm{pp}$ and $f = 200$ kHz is applied to the coil. The grid size is non-uniform, and the minimum grid size is $\Delta r = \Delta z = 10^{-4}$ m in the region of the plasma and around the coil. The grid size is gradually increased towards the axial and radial edges (Fig. 3). The total number of grid cells is 360 axial × 2008 radial.

At the boundaries of the calculation domain of the EM model, the Mur's 1st-order absorbing boundary condition (BC) is applied for the electric field at the axial and radial edges[6]. The axisymmetric BC is used at the axis; the radial and azimuthal components of the EM field are set to be zero.

In this paper, we focus on the behavior of the plasma and EM field at the early stage of the AC applied to the coil in the acceleration phase. In the case of the steady operation of the accelerator as a thruster, the results shown in this paper will appear repeatedly. The calculation including the plasma discharge is the future work for investigating other acceleration mechanism.

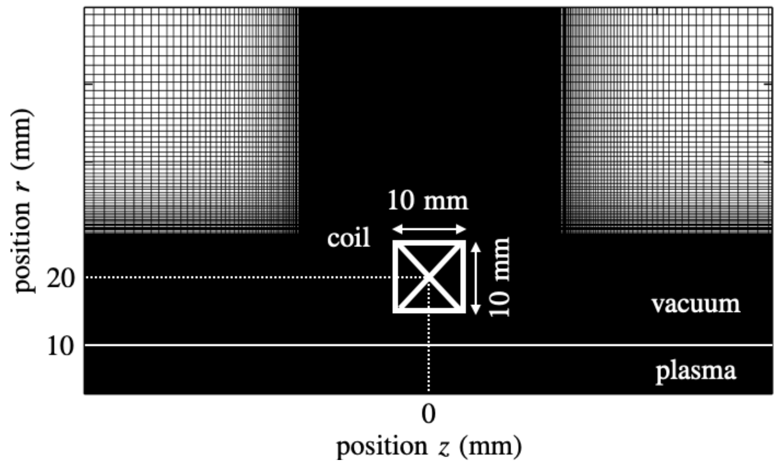

Figure 3. Model geometry of acceleration part of thruster and loop coil.

IV. Results and Discussion

A. Acceleration by Lorentz force

Figure 4 shows the axial distribution of $v_{\mathrm{i},z}$ at 500 ns. The range of the coil is $-0.005 \leq z \leq 0.005$ m. Ions are accelerated to about hundred m/s near the wall of the thruster (r = 8 mm). On the other hand, the increment of the ion velocity is much smaller at the central area of the cylinder. In our model, only the Lorentz force is included as the source which accelerates charged particles; therefore, it is shown numerically that the electromagnetic acceleration by the Lorentz force is dominant at only the surface of the plasma. The past experiment shows that ions are accelerated at even the central region, so other mechanisms, such as electrothermal force, are responsible for the realistic situation.

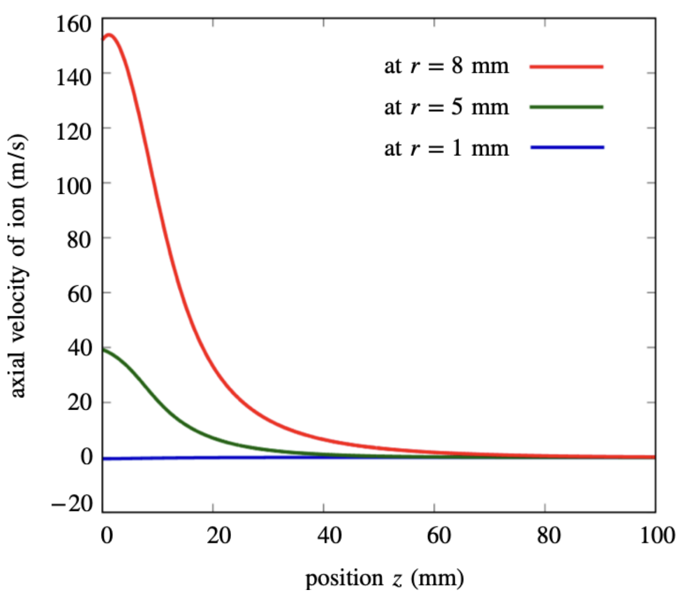

Figure 4. Axial ion velocity at 500 ns.

B. Reversed EM field

The region where electrons are accelerated by $\mathbf{F}_\mathrm{L}$ depends on the depth effected by the EM field, because $\mathbf{F}_\mathrm{L}$ results from the rotating electrons due to the EM induction and $B_{\mathrm{MN},r}$. The distribution of the magnetic vector is shown in Fig. 5. The magnetic field at the central region ($r \leq 6$ mm) is reversed compared with the one near the surface of the plasma. The field reverse is caused when the induced magnetic field due to the rotating motion of electrons becomes larger than penetrating magnetic field generated by the coil at the inside of j_θ-distribution as shown in Fig. 6.

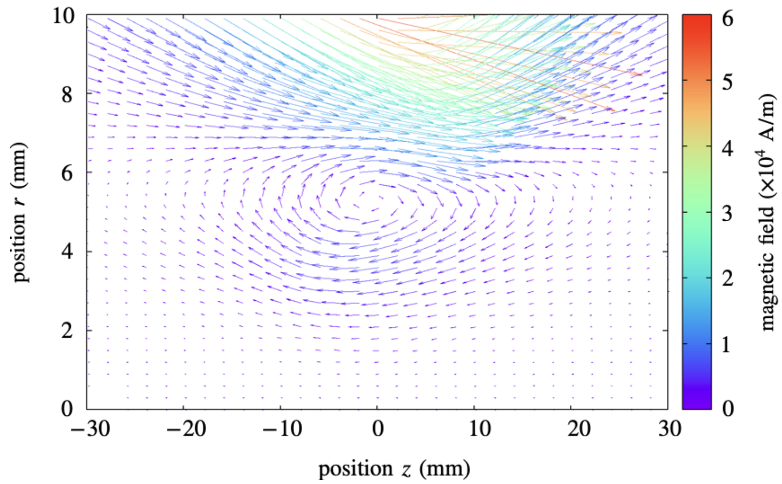

Figure 5. Magnetic field distribution at 500 ns.

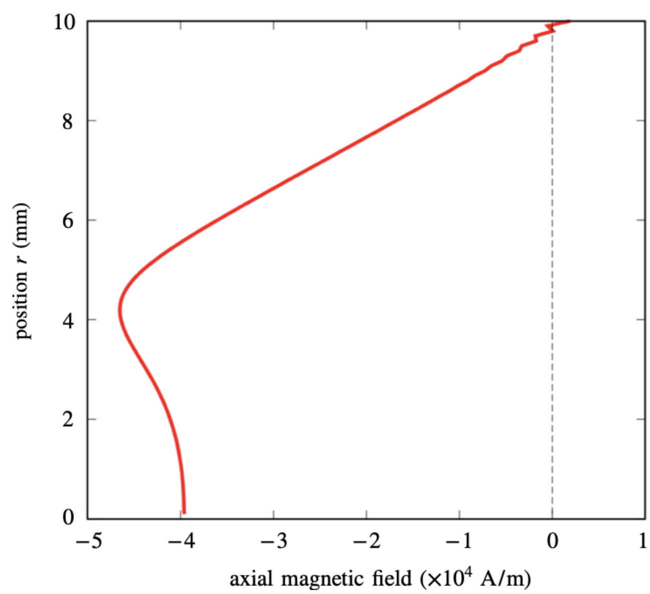

Figure 6. Axial magnetic field induced by rotating electrons.

C. Reversed field area formation

The position where the EM field is reversed may change depending on the skin depth which is determined by the plasma density. In this calculation, axial component of MN is not applied. The dispersion relation of the EM field propagating in the plasma without the static magnetic field is given by

$$\omega^2 = \omega_{\mathrm{p}}^2 + c^2 k^2, \tag{13}$$

where $\omega = 2\pi f$, and $\omega_{\mathrm{p}} = (n_{\mathrm{e}} q^2 / \varepsilon_0 m_{\mathrm{e}})^{1/2}$. In case that f is fixed, k is defined by only the plasma density. Because the plasma density is lower than the cut-off density when the frequency of AC is $\mathcal{O}(\mathrm{kHz})$, the EM field can penetrate in about the skin depth, δ, given by the following equation:

$$\delta = ||k||^{-1} = \frac{c}{\sqrt{\omega_{\mathrm{p}}^2 - \omega^2}}. \tag{14}$$

Substituting plasma densities $n_{\mathrm{e}} = 10^{17}, 10^{18}$, and 10^{19} m^{-3} in Eq. (14), δ becomes $16, 5.0$, and 1.6 mm, respectively. The distribution of $\widetilde{E_\theta}$ at $z = 0$ mm in the plasma is shown in Fig. 7. The length of penetrating $\widetilde{E_\theta}$ at the surface of the plasma is roughly estimated by δ. The field is reversed at $r < 10 - \delta$ in case of $\delta < 10$ mm; on the other hand, the field is not reversed in case of $\delta > 10$ mm. Because the skin depth δ is defined by the plasma density and applied frequency, the radius of the thruster should be chosen according to δ in order to accelerate even the central plasma.

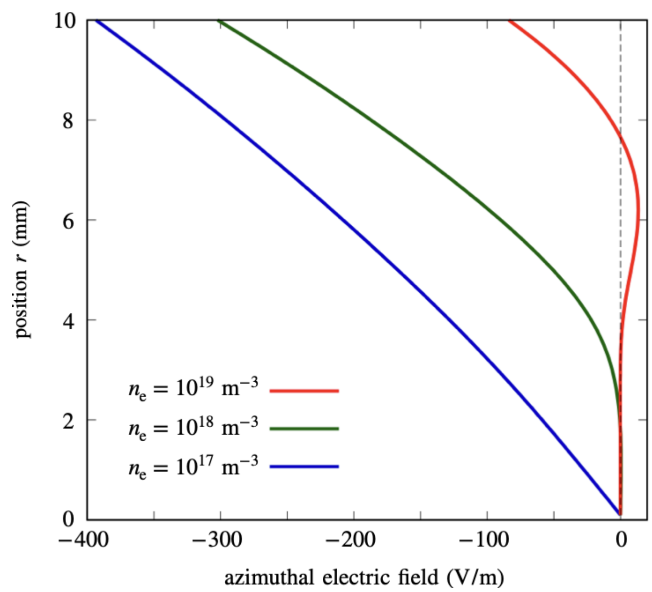

Figure 7. Azimuthal electric field.

V. Conclusion

We have developed a two-dimensional axisymmetric numerical model reproducing a plasma behavior in the electrodeless plasma thruster driven by the loop coil. The plasma fluid simulation coupled with the EM field calculation indicates that the Lorentz force is the main acceleration mechanism at only the surface of the plasma in the thruster. The EM field induced by the j_θ becomes larger at the central region, and the net EM field is finally reversed. This reversed field works as the deceleration factor; therefore, the parameters, such as the plasma density, applied frequency of AC, and radius of thrusters, should be selected for the effective acceleration. For more detailed investigation of the acceleration mechanism, the discharge model will be included as the future work.

References

[1] Bathgate, S. N., Bilek, M. M. M., and Mckenzie, D. R., "Electrodeless Plasma Thrusters for Spacecraft: a Review," *Plasma Sci. Technol.*, Vol. 19, No. 8, 20 Jun. 2017, 083001.

[2] Shinohara, S., Kuwahara, D., Ishii, T., Iwaya, H., Nishimura, S., Yamase, T., Araki, D., and Horita, H., "Development of High-Density Radio Frequency Plasma Sources with Very Small Diameter for Propulsion," *IEEE Trans. on Plasma Sci.*, Vol. 46, No. 2, Feb., 2018, pp. 252–262.

[3] Kuwahara, D., Shinohara, S., Ishii, T., Otsuka, S., Nakagawa, T., Kishi, K., Sakata, M., Tanaka, E., Iwaya, H., Takizawa, K., Tanida, Y., Naito, T., and Yano, K., "High-Density Helicon Plasma Thrusters Using Electrodeless Acceleration Schemes," *Trans. JSASS Aerospace Tech. Japan*, Vol. 14, No. ists30, 28 Jul., 2016, pp. Pb_117–Pb_121.

[4] Yee, K. S., "Numerical solution of initial boundary value problems involving maxwell's equations in isotropic media," *IEEE Trans. AntennasPropag.*, Vol. 14, No. 3, May 1966, pp. 302–307.

[5] Hagelaar, G. J. M., Makasheva, K., Garrigues, L., and Boeuf, J-P., "Modeling of a Dipolar Microwave Plasma Sustained by Electron Cyclotron Resonance," *J. Phys. D: Appl. Phys.*, Vol. 42, 18 Sep., 2009, 194019.

[6] Gerrit Mur, "Absorbing Boundary Conditions for the Finite-Difference Approximation of the Time-Domain Electromagnetic-Field Equations," *IEEE Trans. Electromagn. Compat.*, Vol. EMC-23, No. 4, Nov., 1981, pp. 377–382.